ACS OMEGA

Open Access



http://pubs.acs.org/journal/acsodf

Article

# Secondary Structures of Human Calcitonin at Different Temperatures and in Different Membrane-Mimicking Environments, Characterized by Circular Dichroism (CD) Spectroscopy

Sebastian K.T.S. Wärmländer,*[,#] Amanda L. Lakela,[#] Elina Berntsson, Jüri Jarvet, and Astrid Gräslund*

Cite This: *ACS Omega* 2025, 10, 17133−17142

Read Online

ACCESS | Metrics & More | Article Recommendations

**ABSTRACT:** Human calcitonin is a 32-residue peptide hormone that binds to the calcitonin receptor (CTR) and is involved in calcium regulation. The amino acid sequence displays a hydrophilic central segment flanked by hydrophobic C- and N-terminal regions with a net charge of zero at neutral pH. This makes the molecule amphiphilic and conformationally flexible, and different CTR variants preferentially recognize different structural conformations of calcitonin. The peptide is secreted from the thyroid gland and is overproduced in some forms of thyroid cancer and can then form cell-toxic aggregates. Characterizing the structural properties of calcitonin under different conditions is, therefore, important for understanding its receptor-binding and self-aggregation properties. Here, we used circular dichroism (CD) spectroscopy to monitor the secondary structure of human calcitonin in different environments. Calcitonin monomers were found to display a random coil structure with a significant amount of PPII-helix components in phosphate buffer, pH 7.3, at physiological temperatures. When agitated, the peptide formed soluble aggregates over time with mainly an antiparallel $\beta$-sheet secondary structure. In the presence of micelles of differently charged surfactants, monomeric calcitonin formed a pure $\alpha$-helix structure with cationic CTAB, a combination of $\alpha$-helix and $\beta$-sheet with anionic SDS and with zwitterionic SB3-14, and remained mainly random coil with noncharged DDM. Thus, the charge of the surfactant headgroup was found to be an important parameter for calcitonin's interactions with membrane-mimicking micelles. Similar but not identical interactions with the surfactants were observed under the oxidizing and reducing conditions.

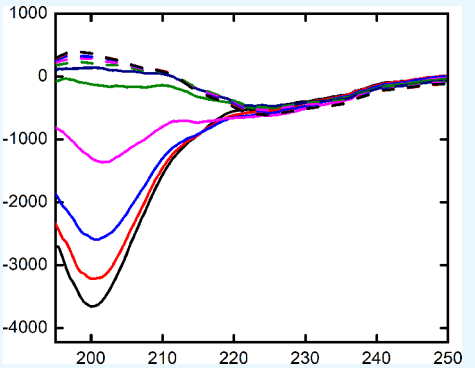


## 1. INTRODUCTION

Human calcitonin is a 32-residue peptide hormone involved in calcium regulation.[1] It is mainly secreted from the parafollicular cells in the thyroid gland.[2] When bound to the calcitonin receptor (CTR), a member of a subfamily of the seven-transmembrane domain G-protein coupled receptor super family,[3] calcitonin activates various signaling pathways to regulate calcium levels.[1,4] For example, the phospholipase enzyme C pathway releases Ca(II) ions from intracellular storages,[5] while the cyclic AMP (cAMP) pathway can affect the motility of osteoclasts via the regulatory protein kinase A (PKA) enzyme.[6] In osteoclasts, calcitonin binding to osteoclast CTR receptors induces contractions that reduce osteoclast motility and thereby prevent them from breaking down bone tissue.[3] Because of these effects, exogenous calcitonin can be used as a therapeutic agent to act against hypercalcemia and to treat metabolic bone diseases such as osteoporosis, osteo-arthritis, and Paget's disease.[1,7] Such treatments typically employ salmon calcitonin, which has a binding affinity for human calcitonin receptors that is 40−50 times stronger than that of human calcitonin.[1,7,8]

A further aspect of calcitonin is its capacity to aggregate into amyloid fibrils, a feature shared with certain other small peptides such as amylin (IAPP), amyloid-$\beta$ (A$\beta$), and insulin.[9−11] The amyloid aggregation process is typically harmful and associated with diseases such as Alzheimer's, Parkinson's, and Creutzfeldt-Jakob.[12,13] In the current view, the most cell-toxic amyloid aggregates are the intermediate soluble oligomers, rather than the mature and insoluble amyloid fibrils that are the final product of the aggregation process.[14,15] Calcitonin aggregation in humans is mostly associated with medullary thyroid carcinoma (MTC), where cancerous growth of the parafollicular cells results in increased calcitonin production.[16] Because the elevated calcitonin concentration does not perfectly correlate with MTC, it is not a reliable marker for the disease.[17] Yet, the thyroids of

**Received:** June 5, 2024
**Revised:** August 9, 2024
**Accepted:** August 21, 2024
**Published:** April 22, 2025

MTC patients typically display amyloid deposits of aggregated calcitonin.[18] Although calcitonin aggregates—especially oligomeric ones—have been shown to be cell-toxic,[19] it is unclear if such toxic aggregates contribute to the MTC pathology and associated thyroid degradation. Similar to other amyloid peptides such as amyloid-$\beta$, calcitonin aggregation is influenced by numerous factors including metal ions.[8,13,20] Aggregation of therapeutic calcitonin in, e.g., storage vials, is a well-known problem, since the aggregates are not only toxic but also less prone to bind to the calcitonin receptor.

To understand the functions and behavior of calcitonin at the molecular level, it is important to understand its structural properties. Such knowledge may facilitate the design of calcitonin-mimicking drugs, which should have a strong affinity for the calcitonin receptor, but not be able to aggregate themselves or to induce aggregation of native calcitonin.[21] In aqueous solution calcitonin generally adopts a random coil secondary structure,[22,23] which is typical for small peptides. When bound to the CTR receptor, salmon calcitonin has been shown to adopt a type II $\beta$-turn conformation.[24] Receptor-bound human calcitonin most likely adopts a similar conformation. When aggregating into amyloid material, calcitonin can adopt a combination of $\alpha$-helix and $\beta$-sheet structures.[22,23]

Here, we used circular dichroism (CD) spectroscopy to characterize the secondary structure of human calcitonin in different environments, by varying temperature, reducing/oxidating environment, and agitating or quiescent conditions and by adding membrane-mimicking and micelle-forming surfactants that are either positively charged, negatively charged, uncharged, or zwitter-ionic.

## 2. MATERIALS

Sodium dodecyl sulfate (SDS), myristyl sulfobetaine (SB3-14), cetyltrimethylammonium bromide (CTAB), dodecyl $\beta$-D-maltoside (DDM), tris(2-carboxyethyl) phosphine (TCEP), and human calcitonin peptide (obtained in vials containing 1 mg of lyophilized peptide powder) were all purchased from Sigma-Aldrich (Germany).

Prior to the experiments, the calcitonin powder was dissolved in Milli-Q water to an approximate concentration of 200 $\mu$M. The exact concentration was determined with a NanoDrop spectrophotometer. The peptide solution was then mixed with 20 mM phosphate buffer, pH 7.3, and diluted to a final concentration in the range 5 $\mu$M−20 $\mu$M. Before the measurements of peptide aggregation kinetics, the calcitonin solution was filtered through a syringe filter membrane with 0.2 $\mu$m pore size (VWR International, USA). This purification step removed large preformed calcitonin aggregates but also reduced the peptide concentration.

## 3. METHODS: CIRCULAR DICHROISM (CD) SPECTROSCOPY

Circular dichroism (CD) is a spectroscopic technique based on the capacity of chiral molecules, including peptides, proteins, and nucleic acids, to interact differently with left- and right-circularly polarized light.[25−28] Peptide bonds, i.e., amide groups in the protein/peptide backbone, have two low-energy electronic transitions that dominate the absorption and CD spectra of peptides and proteins in the far-UV region: the n → $\pi^*$ transition, which is weak in absorption ($\varepsilon_{max} \sim 100$ L·M$^{-1}$·cm$^{-1}$) but often strong in CD around 220 nm, and the $\pi \rightarrow \pi^*$ transition around 190−200 nm, which is strong in both absorption ($\varepsilon_{max} \sim 7.000$ L·M$^{-1}$·cm$^{-1}$) and CD.[26,28]

Because CD spectra for peptide bonds are influenced by the geometries of the protein/peptide backbone, such CD spectra reflect the different types of secondary structures that are present.[25−28] Figure 1 shows typical CD spectra for four model

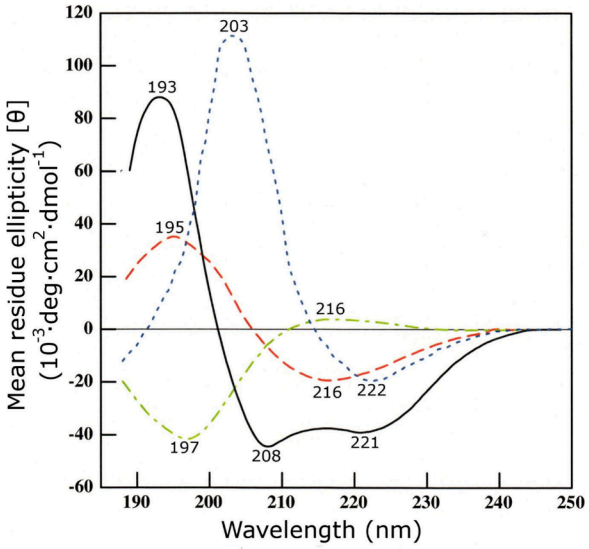


**Figure 1.** Circular dichroism (CD) spectra of four model secondary structures. Polylysine ($Lys_n$, $M_r$ = 193.000) is an $\alpha$-helix (black solid line) at pH 10.8 and 25 °C in water; an antiparallel $\beta$-sheet (red dashed line) at pH 11 after heating for 15 min at 52 °C and cooling back to 25 °C; and a random coil (green dashed dotted line) at neutral pH.[36] The BOC(L-Val)$_7$OMe oligopeptide as a thin film is in a parallel $\beta$-sheet (blue dashed line) conformation.[37] The figure is adapted with permission from Figure 4 in Jarvet (1999),[26] where the copyright belongs to J. Jarvet.

secondary structures, i.e., $\alpha$-helix, parallel $\beta$-sheet, antiparallel $\beta$-sheet, and random coil.[26] Characteristic features include the wavelengths for minima, maxima, and the $x$-axis intercept. For example, CD spectra for the $\alpha$-helix secondary structure usually have minima around 208 and 222 nm and intercept the $x$-axis slightly above 200 nm (Figure 1).

Various algorithms have been developed for estimating from CD spectra the proportions of different secondary structure components, such as the BeStSel,[29] CAPITO,[30] and CDtoolX[31] software. However, in certain situations, such analysis can be difficult, as different secondary structures may sometimes produce very similar CD spectra. For example, it is well established that disordered proteins and peptides display characteristic CD spectra with a strong minimum around 200 nm and a low amplitude around 222 nm.[32−35] But this type of CD spectrum can also be obtained for globular proteins rich in highly twisted antiparallel $\beta$-sheets, such as ferredoxin and dUTP pyrophosphatase.[35] In such situations, other techniques such as nuclear magnetic resonance (NMR) spectroscopy and X-ray crystallography might be required for obtaining accurate structural information.[32]

The "random coil" conformation is not a unique secondary structure, but rather a statistical distribution of different conformations that a polypeptide will adopt in the absence of specific stabilizing interactions.[38] One of these conformations is the extended left-handed polyproline II (PPII) helix, which can be identified with CD spectroscopy.[33,39] The PPII helix


https://doi.org/10.1021/acsomega.4c05312
ACS Omega 2025, 10, 17133−17142

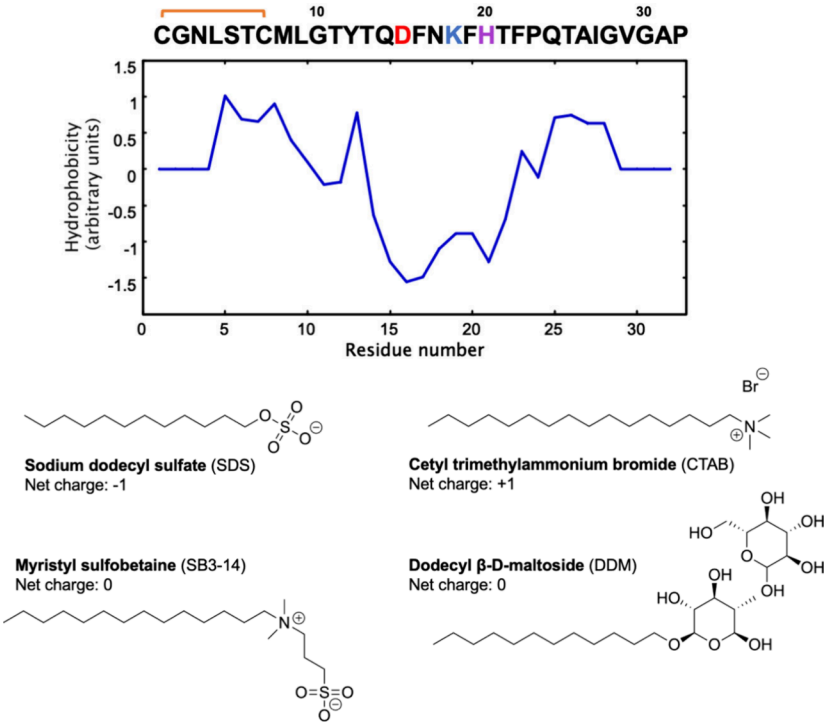


**Figure 2.** Top: Sequence and hydrophobicity profile of human calcitonin. Potentially charged residues are colored. The orange line shows an S−S link between Cys1 and Cys7. Bottom: chemical structures of the micelle-forming surfactants sodium dodecyl sulfate (SDS), cetyltrimethylammonium bromide (CTAB), myristyl sulfobetaine (SB3-14), and dodecyl $\beta$-D-maltoside (DDM).

lacks internal hydrogen bonding and is relatively common in intrinsically disordered and unstructured proteins and peptides.[40,41] In a polypeptide that is mainly random coil, the amount of PPII helix present can be estimated (in percent) from a CD spectrum via eq 1:[33]

$$\%\text{PPII helix} = \frac{[\theta]\text{max} + 6100}{13700} \times 100 \quad (1)$$

Here, −6100 deg·cm$^2$·dmol$^{-1}$ is the theoretical ellipticity for the 0% PPII helix. $[\theta]_{max}$ is the measured CD signal intensity, in units of molar ellipticity, at the local maximum around 220−225 nm, where the exact position of the maximum varies between different peptides.[32,33]

In the current study, a Chirascan CD spectrometer (Applied Photophysics, UK) was used to record CD spectra of 5−20 $\mu$M human calcitonin in 20 mM phosphate buffer, pH 7.3, under different conditions. The sample chamber of the spectrometer was equipped with a magnet for stirring and a Peltier element for temperature control. The latter was connected to a TC 425 temperature controller (Quantum Northwest, USA). Calcitonin samples were analyzed in quartz cuvettes with path lengths of either 1 mm (300 $\mu$L volume), 2 mm (600 $\mu$L volume), or 4 mm (1200 $\mu$L volume). CD spectra were recorded between 195 and 250 nm, with a step size of 0.5 nm and a sampling time of 7 s per data point, yielding a recording time of 14 min per spectrum.

The effect of temperature on the calcitonin secondary structure was studied under both quiescent and agitating (i.e., stirring) conditions. The amount of PPII helix was evaluated according to eq 1, where the local PPII maximum was found to be at 221 nm for the calcitonin peptide. The overall proportions of $\alpha$-helix, parallel and antiparallel $\beta$-sheets, $\beta$-turns, and other secondary structure elements were estimated by the BeStSel algorithm,[29] by uploading CD spectra to the bestsel.elte.hu Web site.

To investigate the secondary structure of calcitonin in different membrane-mimicking environments, samples were titrated with micelle-forming surfactants (Figure 2) that were positively charged (CTAB), negatively charged (SDS), zwitterionic (SB3-14), or uncharged (DDM). These measurements were conducted at 25 °C, at surfactant concentrations that were both below and above the critical micelle concentration (cmc) for each surfactant. For the four studied surfactants, the cmc values and the number of molecules ($n$) that form one micelle (at temperatures around 20−25 °C) are the following:[42] for SDS, cmc is 7−10 mM and $n$ is 62; for CTAB, cmc is 0.9−1 mM and $n$ is 61; for SB3-14, cmc is 0.1−0.4 mM and $n$ is 83; and for DDM, cmc is 0.15 mM and $n$ is 98. Most measurements were performed in a standard oxidizing environment. However, in some experiments with SDS and CTAB, 1 mM TCEP was added to the sample to create a reducing environment that would break the intrinsic N-terminal S−S-bridge of calcitonin (Figure 2).

## 4. RESULTS

**4.1. Effect of Temperature on Calcitonin Secondary Structure.** Monomeric calcitonin in aqueous solution was found to display a CD spectrum with a characteristic minimum around 198 nm (Figure 3A), typical of the random coil secondary structure (Figure 1). Increasing the temperature from 5 to 55 °C in increments of 5 °C, without stirring or otherwise agitating the sample, induced a structural transition with an isodichroic point around 207 nm. Figure 3A shows the spectra for this experiment at 10 °C intervals. When the temperature was gradually decreased back to 5 °C, the same structural transition and isodichroic point at 207 nm was


https://doi.org/10.1021/acsomega.4c05312
ACS Omega 2025, 10, 17133−17142

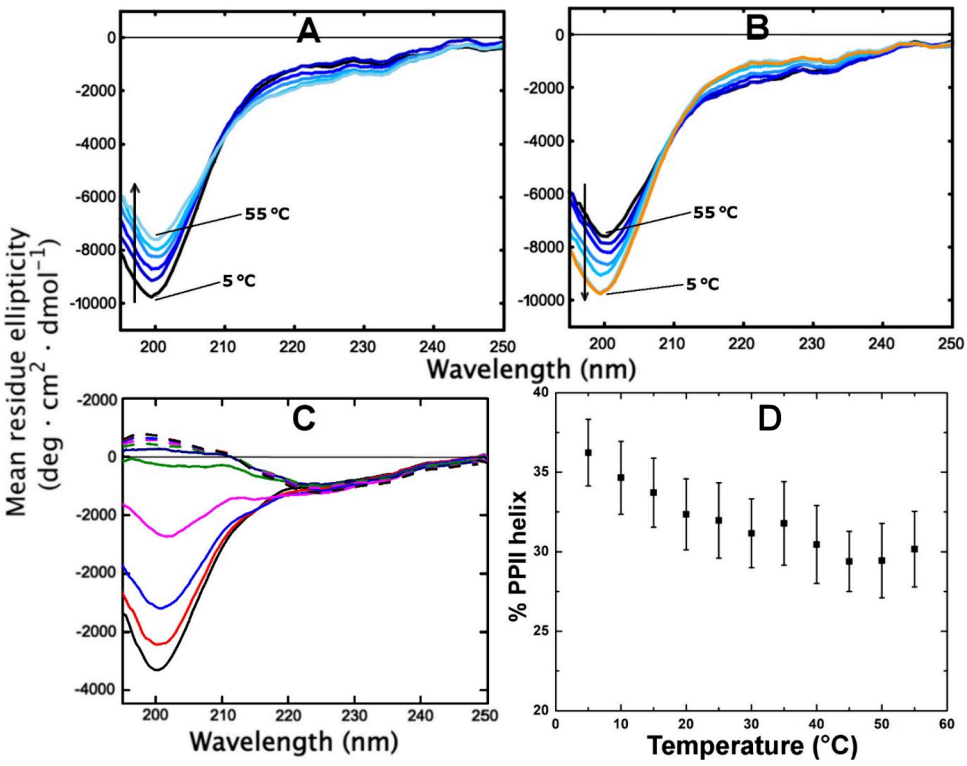


**Figure 3.** (A, B) CD spectra of 15 $\mu$M monomeric calcitonin in 20 mM phosphate buffer, pH 7.3, at different temperatures. The spectra ranging from black to light blue in (A) are measured from 5 to 55 °C, in 10 °C increments without stirring the sample. The curves ranging from black to light blue in (B) are measured from 55 to 5 °C, in 10 °C increments without stirring the sample. The spectrum recorded at 5 °C at the beginning of the temperature measurements is shown in orange. (C) CD spectra of 5 $\mu$M calcitonin in 20 mM phosphate buffer, pH 7.3, were recorded at different temperatures while the sample was continuously agitated with a magnetic stirrer. First, black, red, blue, pink, green, and violet spectra were recorded when the temperature was increased from 5 to 55 °C, in 10 °C increments. Then, dashed violet, green, pink, blue, red, and black spectra were recorded when the temperature was decreased from 55 °C back to 5 °C, in 10 °C increments. (D) Amount of PPII helix in the calcitonin secondary structure, calculated from the CD intensities at 221 nm according to eq 1, and plotted against temperature at intervals of 5 °C. The error bars show standard deviations calculated from four repeats.

observed, and the final spectrum at 5 °C was the same as that at the beginning of the experiment (Figure 3B). This showed that the observed temperature-induced structure transition was completely reversible.

The loss of CD signal intensity at the 198 nm minimum and the increased signal around 215−230 nm, together with the isodichroic point around 207 nm (Figure 3A), indicated that the structural transition involves a loss of polyproline II (PPII) helix structure at elevated temperatures.[32,43] It has previously been argued that for monomers of intrinsically disordered proteins and peptides, such temperature-induced changes in CD signal intensity around 200 and 220 nm typically correspond to a redistribution of random coil elements including the PPII helix,[43] as shown for, e.g., A$\beta$ peptides.[32] Thus, the amount of PPII helix present at each temperature was calculated from eq 1,[33] using the CD intensity at 221 nm. An almost linear dependence on temperature was observed (Figure 3D), which is consistent with previous studies.[32,44] These results showed that monomeric human calcitonin displays a fair amount of PPII helix structure in aqueous solution, i.e., around 36% at 5 °C and around 30% at 50 °C.

Figure 3C shows CD spectra for calcitonin, recorded while the sample was continuously stirred by a magnetic stirrer and the temperature was stepwise increased, from 5 to 55 °C and back again in 10 °C increments. Here, the sample clearly transitioned into a rather pure antiparallel $\beta$-sheet structure at high temperatures, with a characteristic broad minimum between 220 and 230 nm (Figure 1). It should be noted that in the 225 nm−250 nm region, the CD spectra are very similar for calcitonin in random-coil conformation and in aggregated antiparallel $\beta$-sheet conformation (Figure 3C). Thus, very small spectral changes are observed in this region when the sample aggregates. The structural transition was found to be irreversible, as the sample stayed in the $\beta$-sheet conformation also when the temperature was gradually reduced back to 5 °C (Figure 3C). This is not surprising, as both increasing the temperature and agitating (stirring) the sample is known to promote amyloid aggregation, which typically takes place with the protein or peptide in $\beta$-sheet conformation. Furthermore, it is well-known that amyloid aggregation processes are generally difficult to reverse. The spectra in Figure 3C therefore appear to correspond to gradual aggregation of the calcitonin sample into soluble and stable amyloid aggregates with a $\beta$-sheet structure.

**4.2. Temperature Dependence of Calcitonin Aggregation Kinetics.** To further explore the effects of temperature on calcitonin aggregation, CD spectra were recorded when calcitonin samples were continuously stirred at constant temperatures of 10 °C, 25 °C, or 37 °C, respectively (Figure 4). At all three temperatures, the CD spectra displayed gradual structural transitions (Figure 4) from a random coil conformation (minimum at 198 nm) to an antiparallel $\beta$-sheet conformation (minimum around 225 nm). The transition rate was fastest at 37 °C, where the $\beta$-sheet structure


https://doi.org/10.1021/acsomega.4c05312
ACS Omega 2025, 10, 17133−17142

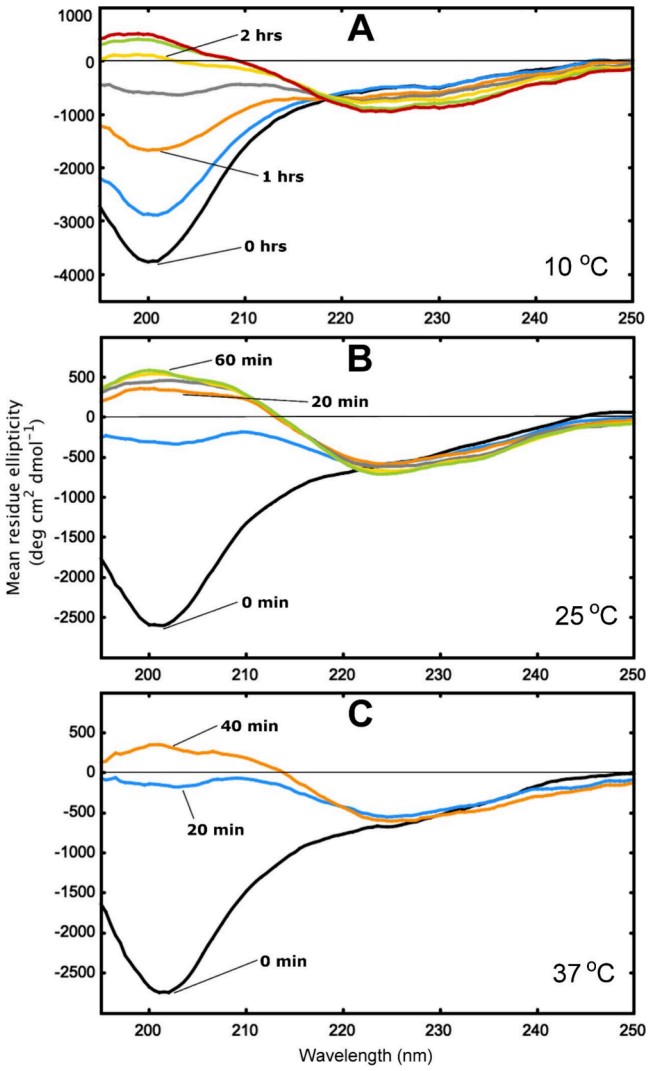


**Figure 4.** CD spectra showing the aggregation kinetics of human calcitonin at different temperatures. Spectra were recorded at different time points for 5 $\mu$M calcitonin in 20 mM phosphate buffer, pH 7.3, when the samples were continuously stirred at different temperatures. (A) 10 °C at 0 h (black), 0.5 h (blue), 1 h (orange), 1.5 h (gray), 2 h (yellow), 2.5 h (green), and 3 h (red). (B) 25 °C at 0 min (black), 10 min (blue), 20 min (orange), 30 min (gray), 45 min (yellow), and 60 min (green). (C) 37 °C at 0 min (black), 20 min (blue), and 40 min (orange).

formed after 20 min (Figure 4C), and slowest at 10 °C, where it took 150 min for the $\beta$-sheet structure to fully form (Figure 4A). At 25 °C, the $\beta$-sheet conformation was reached after 40 min (Figure 4B). Thus, as expected, increasing the temperature clearly promoted calcitonin aggregation via antiparallel $\beta$-sheet interactions.

**4.3. Effects of Micelles of Different Surfactants on Calcitonin Secondary Structure.** CD spectroscopy was also used to study the effects of different surfactants, i.e., SDS, CTAB, SB3-14, and DDM (Figure 2), on the secondary structure of 20 $\mu$M monomeric calcitonin in 20 mM phosphate buffer at pH 7.3, 25 °C (Figure 5). Measurements were conducted both below and above the critical micelle concentration (cmc) of the surfactants. As calcitonin in phosphate buffer adopts a random coil, this was the starting point for all titration series.

Stepwise addition of negatively charged SDS molecules, up to 8 mM, which is around the cmc value for SDS, induced clear and systematic changes in the CD spectra that correspond to a structural transition into a combination of $\alpha$-helix and $\beta$-sheet structure (Figure 5A). This interpretation is based on comparisons with almost identical CD spectra previously recorded for aggregated calcitonin, where the structure was identified as combined $\alpha$-helix and $\beta$-sheet.[22,23] Earlier work has shown that SDS is a good membrane model for amyloidic peptides such as A$\beta$,[45] and that such peptides in complex with SDS adopt similar structures as they do in aggregated or oligomeric form.[46,47] It is therefore not surprising that calcitonin in SDS displayed a secondary structure similar to that of aggregated calcitonin.

A transition into the same type of conformation with mixed $\alpha$-helix and $\beta$-sheet structure was observed also for calcitonin titrated with the zwitterionic surfactant SB3-14, up to 3 mM concentration, which is well above the cmc value for SB3-14 (Figure 5C). When calcitonin was titrated with the positively charged CTAB molecule, a similar transition into a combination of $\alpha$-helix and $\beta$-sheet structures was observed for CTAB concentrations below cmc (Figure 5B). However, upon addition of 1 mM CTAB, which is just above the cmc value, a typical $\alpha$-helical CD spectrum was induced with characteristic minima at 208 and 222 nm (Figure 5B). Additions of the noncharged DDM surfactant induced only minor changes in the CD spectrum, i.e., a slight loss of signal intensity and a slight shift of the minimum toward shorter wavelengths (Figure 5D). These spectral changes were much smaller than those induced by the other surfactants, indicating that DDM has weaker effects on the secondary structure of calcitonin. Thus, it is clear that the interactions between calcitonin and surfactants are strongly influenced by the charge of the surfactant headgroup.

Titrations of the surfactants SDS and CTAB to calcitonin were also performed in the presence of 1 mM reducing agent TCEP (Figure 6). This concentration roughly corresponds to the reducing environment inside human cells. First, a CD spectrum of calcitonin at neutral pH under standard oxidizing conditions was recorded, showing the same random coil signal as that observed in the earlier measurements. Upon addition of TCEP, the CD spectrum lost some intensity and the minimum at 298 nm shifted slightly toward shorter wavelengths (Figure 6). As the main effect of a reducing environment is to break the S−S-bridge between calcitonin residues Cys1 and Cys7 (Figure 2), this observation showed that the N-terminal S−S-bridge is important for calcitonin secondary structure.

Addition of up to 8 mM SDS under reducing conditions produced CD spectra (Figure 6A) that are very similar to those produced under oxidizing conditions (Figure 5A), indicating that calcitonin adopted the same secondary structure with mixed $\alpha$-helix and $\beta$-sheet. The titrations with CTAB yielded an $\alpha$-helical CD signal under reducing conditions (Figure 6B) similar to that obtained under oxidizing conditions (Figure 5B). However, the $\theta_{222}/\theta_{208}$ ratio is 0.61 under reducing conditions (Figure 6B) and 0.77 under oxidizing conditions (Figure 5B). In $\alpha$-helix structures the $\theta_{222}/\theta_{208}$ ratio is known to reflect helix supercoiling, i.e., when two or more $\alpha$-helices form coiled coils via hydrophobic interactions,[48−50] and where $\theta_{222}/\theta_{208}$ ratios close to 1 indicate large amounts of superhelicity.[51] Such coil−coil interactions can be induced in membrane environments, but also be external factors such as metal ions.[52,53] Overall, the small but distinct differences in the


https://doi.org/10.1021/acsomega.4c05312
ACS Omega 2025, 10, 17133−17142

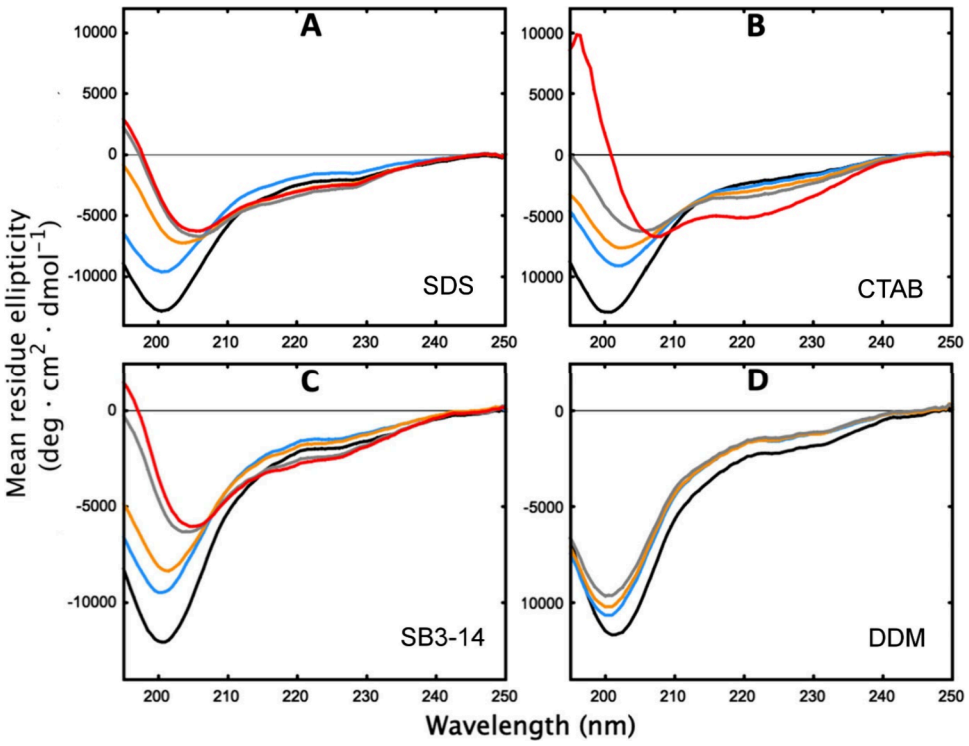


**Figure 5.** CD spectra of 20 $\mu$M monomeric calcitonin in 20 mM phosphate buffer, pH 7.3 (black spectra), titrated with different surfactants at 25 °C. (A) SDS in amounts of 900 $\mu$M (blue), 1.2 mM (orange), 1.5 mM (gray), and 8 mM (red). (B) CTAB in amounts of 25 $\mu$M (blue), 100 $\mu$M (orange), 200 $\mu$M (gray), and 1 mM (red). (C) SB3-14 in amounts of 100 $\mu$M (blue), 300 $\mu$M (orange), 1 mM (gray), and 3 mM (red). (D) DDM in amounts of 100 $\mu$M (blue), 500 $\mu$M (orange), and 1 mM (gray).

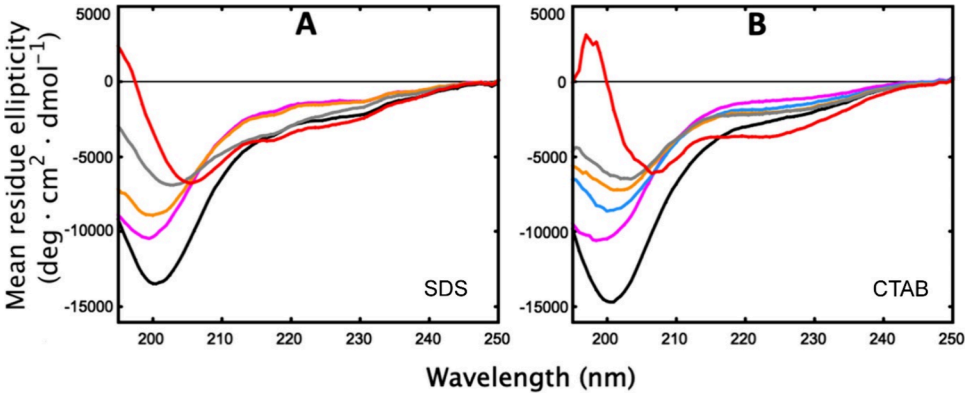


**Figure 6.** CD spectra of 20 $\mu$M monomeric calcitonin in 20 mM phosphate buffer, pH 7.3 at 25 °C, in a standard oxidizing environment (black spectra) and after addition of 1 mM TCEP (magenta spectra). (A) Titration with SDS was done in amounts of 300 $\mu$M (orange), 400 $\mu$M (gray), and 8 mM (red). (B) Titration with CTAB was carried out in amounts of 25 $\mu$M (blue), 100 $\mu$M (orange), 200 $\mu$M (gray), and 1 mM (red).

structural effects induced by SDS and CTAB in oxidizing and reducing conditions, respectively, showed that the N-terminal S−S bridge (Figure 2), which is disrupted in a reducing environment, is important for some aspects of the calcitonin secondary structure.

## 5. DISCUSSION

The secondary structure conformations adopted by the calcitonin peptide naturally influence its biomolecular interactions, such as receptor binding and self-aggregation. As an amphiphilic and conformationally flexible molecule, with a zero net charge at neutral pH and a hydrophilic central segment flanked by hydrophobic C- and N-terminal regions (Figure 2), monomeric human calcitonin often adopts a random coil structure in aqueous solution.[22,23,54] The N-terminal region may however sometimes adopt a $\beta$-sheet conformation.[55] At acidic pH, the C-terminal region can adopt a $\beta$-sheet conformation, while the N-terminal region can form an $\alpha$-helical structure stabilized by the Cys1-Cys7 S−S bridge (Figure 2).[55] In nonaqueous solutions containing, e.g., trifluoroethanol (TFE) or methanol, human calcitonin can adopt $\alpha$-helical structures also at neutral pH.[56,57] Salmon calcitonin, which differs from human calcitonin in 16 out of 32 amino acids, has a less hydrophobic C-terminal region, a higher propensity for $\alpha$-helical secondary structure, and is less prone to aggregate.[22,56,58] In 90% dimethyl sulfoxide (DMSO) with 10% $H_2O$, monomers of both human and salmon calcitonin were reported to adopt an intramolecular $\beta$-sheet hairpin


https://doi.org/10.1021/acsomega.4c05312
ACS Omega 2025, 10, 17133−17142

structure,[59,60] similar to the conformation identified as important for aggregation of Aβ peptides.[11]

Given the capacity of calcitonin to form cell-toxic amyloid aggregates,[19] for example, when overproduced as a result of, e.g., thyroid cancer,[16] the aggregation properties of the peptide are of particular importance.[61] In general, clarifying the structure and toxic mechanisms of oligomers of various peptides and proteins remains an important research task.[15] While most polypeptides adopt β-sheet structure during amyloid aggregation,[11] sometimes amyloid can form via aggregation of α-helical structures.[62,63]

Earlier work has shown that calcitonin can adopt different structures when it is aggregating. For example, aggregates with a combination of both α-helix and β-sheet structure have been observed.[22,23] An aggregation mechanism was suggested where the C-terminal 23−32 residues first form intermolecular β-sheets, which then act as a template for aggregation of α-helical rods comprising residues 8−22.[23] Another study found that human calcitonin aggregated into a mixture of antiparallel and parallel β-sheets at pH 3.3, but into a mixture of antiparallel β-sheets and random coil structure at pH 7.5.[55] Furthermore, an extended version of human calcitonin with an additional N-terminal Leu residue and a C-terminal Gly residue was found to mainly aggregate into β-sheet conformation.[22]

Here, we report that human calcitonin forms an antiparallel β-sheet structure when aggregating in phosphate buffer at pH 7.3 (Figures 3C and 4). Earlier studies have shown that calcitonin aggregation is promoted by various factors, such as increased peptide concentration and temperature,[23] and also by reducing the N-terminal S−S bridge which otherwise stabilizes the N-terminal region.[55,61] Our current results confirm that calcitonin aggregates faster at higher temperatures (Figure 4). They also demonstrate the importance of agitation for the aggregation process, as much stronger temperature-induced aggregation was observed in the samples that were magnetically stirred (Figure 3).

In the samples that were not magnetically stirred, gradually increasing the temperature from 5 to 55 °C induced a structural conversion involving loss of PPII-helix (Figures 3A and 3D). This structural change was found to be completely reversible when the temperature slowly returned to 5 °C (Figure 3B). The presence of PPII-helix in the monomer structure is noteworthy. Human calcitonin has previously been shown to adopt a PPII-helix structure at −85 °C, in the cryogenic solvent ethanediol/water (2:l ratio), while salmon calcitonin under those conditions adopted an α-helical structure.[56] Here, we observe a roughly linear dependence of the amount of PPII-helix structure with temperature and demonstrate that almost 36% PPII-helix component is present in human calcitonin at physiological temperatures (Figure 3D).

Our observations here are in line with earlier studies showing that short peptides often display PPII-helix conformations.[40,41] For example, measurements with CD spectroscopy showed that the full-length Aβ(1−40) peptide adopted around 45% PPII-helix at 0 °C, in 10 mM sodium phosphate buffer at pH 7.4, while the shorter Aβ(1−9) fragment displayed almost 60% PPII-helix under the same conditions.[32] Increasing the temperature to 60 °C induced conversions from high PPII content to mainly a random coil structure. Interestingly, NMR spectroscopy indicated intermediate states around 20 °C involving β-sheet secondary structures.[32] These intermediate states could be important for aggregation processes, as Aβ peptides in antiparallel β-sheet conformation appear to be the building blocks when forming amyloid fibrils,[11] while the PPII-helix conformation seems less suitable for amyloid aggregation.[32]

Similar secondary structure effects could be involved in calcitonin amyloid aggregation. A recent computer simulation study employing all-atom discrete molecular dynamics (DMD) found that during oligomerization, human calcitonin first transitioned from unstructured to helical secondary structure, and then from helical to β-sheet conformation.[64] It was also noted that the transient coil and sheet structures formed in the monomeric peptides were important for the aggregation properties. For the temperature-related loss of PPII helix observed in the current study (Figure 3D), it is unclear if the PPII structure converts into a β-sheet structure or into other types of random coil structure. Figure 3C shows that certain antiparallel β-sheet calcitonin structures produce almost identical CD signals in the 225−250 nm region as the random coil conformation. Thus, CD spectroscopy alone might not be able to accurately identify all different secondary structure components of calcitonin in every situation. According to the BeStSel (Beta Structure Selection) algorithm,[29] the CD spectra of calcitonin in buffer shown in Figures 3A and 3B correspond to around 30% antiparallel β-strand, 0% parallel β-strand, 3% α-helix, 15% β-turn, and 51% random coil elements ("other structures"), irrespective of temperature. This would suggest that the loss of the PPII helix at elevated temperatures (Figure 3D) is caused by a redistribution among random coil elements. But, given the just mentioned spectral overlap in the 225−250 nm region, the results from the BeStSel algorithm should be considered somewhat uncertain.

In addition to aggregation processes, the amount of PPII structure in calcitonin could also be relevant for receptor interactions. Several studies have reported the existence of different variants of calcitonin receptors, with different affinities for helical and nonhelical calcitonin conformations. For example, experiments on rats showed that calcitonin analogues that do not easily adopt α-helical structure selectively recognized calcitonin receptors in bone tissue, whereas α-helical calcitonin analogues seemed to prefer receptors in kidney.[65]

As calcitonin receptors are membrane proteins, it becomes relevant to study calcitonin in membrane-like environments.[4,19,56−58] Membrane interactions, including membrane disruption, could also be involved in the toxic mechanisms of oligomeric aggregates of calcitonin and other amyloidic proteins and peptides.[19,66]

Micelle-forming surfactants are simple membrane models that can be used to investigate basic properties of membrane−peptide interactions, including structure induction.[42,45,67] Here, we show that human calcitonin adopts a combination of α-helix and β-sheet secondary structures in the presence of micelles of anionic SDS (Figure 5A) and zwitterionic SB3-14 (Figure 5C) surfactants. It has previously been shown that salmon calcitonin in SDS micelles displays overall α-helix confirmation.[57,58] For human calcitonin in SDS, a previous study has reported generally similar CD spectra as those presented in Figure 5A, which then were interpreted as reflecting only small amounts (<15%) of α-helix structure.[57] This is compatible with our interpretation of the spectrum as a combination of α-helix and β-sheet structures (Figure 5A). The current results therefore confirm previous reports that human calcitonin is less prone to adopt α-helical structure than salmon calcitonin.[57,58] Here, pure α-helical structure is


https://doi.org/10.1021/acsomega.4c05312
ACS Omega 2025, 10, 17133−17142

observed for human calcitonin monomers only in the presence of micelles of the cationic CTAB surfactant (Figure 5B).

The CD spectra for calcitonin in CTAB are somewhat different in oxidizing and reducing conditions (Figures 5B and 6B), which confirms earlier reports that the calcitonin S−S bridge (Figure 2) is important for N-terminal $\alpha$-helix structure, i.e., by stabilizing it.[55,61] In the presence of noncharged DDM micelles, only minor structural changes are observed, presumably toward more random coil structure. Taken together, these results show that the headgroup charge is an important parameter for surfactant/calcitonin interactions. As biological membranes consist of a multitude of lipids with different properties, including differences in charge,[68−70] the results presented here are likely important for understanding biological calcitonin-membrane interactions.

## 6. CONCLUSIONS

We here show that human calcitonin displays a random coil structure with a significant amount of PPII-helix component in phosphate buffer, pH 7.3, at physiological temperatures. When agitated under these conditions, calcitonin can form soluble aggregates over time that mainly display a $\beta$-sheet secondary structure. In the presence of micelles of differently charged surfactants, monomeric calcitonin forms a pure $\alpha$-helix structure with cationic CTAB, forms a combination of $\alpha$-helix and $\beta$-sheet with anionic SDS and zwitterionic SB3-14, and remains mainly random coil with noncharged DDM. These results improve our understanding of how calcitonin can interact with membranes, which has implications for how monomeric calcitonin binds to membrane receptors and for how aggregated calcitonin induces membrane damage.

## AUTHOR INFORMATION


### Corresponding Authors

**Astrid Gräslund** − *Chemistry Section, Arrhenius Laboratories, Stockholm University, 114 19 Stockholm, Sweden; CellPept Sweden AB, 118 47 Stockholm, Sweden*; Email: astrid@dbb.su.se

**Sebastian K.T.S. Wärmländer** − *Chemistry Section, Arrhenius Laboratories, Stockholm University, 114 19 Stockholm, Sweden; CellPept Sweden AB, 118 47 Stockholm, Sweden*; orcid.org/0000-0003-3917-1838; Email: seb@student.su.se

### Authors

**Amanda L. Lakela** − *Chemistry Section, Arrhenius Laboratories, Stockholm University, 114 19 Stockholm, Sweden*

**Elina Berntsson** − *Chemistry Section, Arrhenius Laboratories, Stockholm University, 114 19 Stockholm, Sweden; CellPept Sweden AB, 118 47 Stockholm, Sweden; Department of Chemistry and Biotechnology, Tallinn University of Technology, 19086 Tallinn, Estonia*; orcid.org/0000-0002-7544-092X

**Jüri Jarvet** − *Chemistry Section, Arrhenius Laboratories, Stockholm University, 114 19 Stockholm, Sweden; CellPept Sweden AB, 118 47 Stockholm, Sweden; The National Institute of Chemical Physics and Biophysics, 12618 Tallinn, Estonia*; orcid.org/0000-0002-7863-1887

Complete contact information is available at: https://pubs.acs.org/10.1021/acsomega.4c05312

### Author Contributions

#S.K.T.S.W. and A.L.L. are co-first authors.


### Notes

The authors declare the following competing financial interest(s): None. A.G., E.B., J.J., and S.K.T.S.W. are shareholders of CellPept Sweden AB. Neither this company, nor the funding organizations, had any role in the design of the study; in the collection, analyses, or interpretation of data; in the writing of the manuscript; or in the decision to publish the results.

## ACKNOWLEDGMENTS

We thank Teodor Svantesson for helpful discussions. The study was supported by grants to A.G. from the Brain Foundation in Sweden and the Swedish Research Council.

## REFERENCES


(1) Srinivasan, A.; Wong, F. K.; Karponis, D. Calcitonin: A useful old friend. *J. Musculoskelet Neuronal Interact* **2020**, *20* (4), 600−609.

(2) Felsenfeld, A. J.; Levine, B. S. Calcitonin, the forgotten hormone: does it deserve to be forgotten? *Clin Kidney J.* **2015**, *8* (2), 180−7.

(3) Masi, L.; Brandi, M. L. Calcitonin and calcitonin receptors. *Clin Cases Miner Bone Metab* **2007**, *4* (2), 117−122.

(4) Garelja, M. L.; Hay, D. L. A narrative review of the calcitonin peptide family and associated receptors as migraine targets: Calcitonin gene-related peptide and beyond. *Headache* **2022**, *62* (9), 1093−1104.

(5) Pondel, M. Calcitonin and calcitonin receptors: bone and beyond. *Int. J. Exp Pathol* **2000**, *81* (6), 405−22.

(6) Suzuki, H.; Nakamura, I.; Takahashi, N.; Ikuhara, T.; Matsuzaki, K.; Isogai, Y.; Hori, M.; Suda, T. Calcitonin-induced changes in the cytoskeleton are mediated by a signal pathway associated with protein kinase A in osteoclasts. *Endocrinology* **1996**, *137* (11), 4685−90.

(7) Xie, J.; Guo, J.; Kanwal, Z.; Wu, M.; Lv, X.; Ibrahim, N. A.; Li, P.; Buabeid, M. A.; Arafa, E. A.; Sun, Q. Calcitonin and Bone Physiology: In Vitro, In Vivo, and Clinical Investigations. *Int. J. Endocrinol* **2020**, *2020*, 3236828.

(8) Rastogi, N.; Mitra, K.; Kumar, D.; Roy, R. Metal ions as cofactors for aggregation of therapeutic peptide salmon calcitonin. *Inorg. Chem.* **2012**, *51* (10), 5642−50.

(9) Raimundo, A. F.; Ferreira, S.; Martins, I. C.; Menezes, R. Islet Amyloid Polypeptide: A Partner in Crime With Abeta in the Pathology of Alzheimer's Disease. *Front Mol. Neurosci* **2020**, DOI: 10.3389/fnmol.2020.00035.

(10) Noormägi, A.; Valmsen, K.; Tougu, V.; Palumaa, P. Insulin Fibrillization at Acidic and Physiological pH Values is Controlled by Different Molecular Mechanisms. *Protein J.* **2015**, *34* (6), 398−403.

(11) Abelein, A.; Abrahams, J. P.; Danielsson, J.; Gräslund, A.; Jarvet, J.; Luo, J.; Tiiman, A.; Wärmländer, S. K. T. S. The hairpin conformation of the amyloid beta peptide is an important structural motif along the aggregation pathway. *J. Biol. Inorg. Chem.* **2014**, *19* (4−5), 623−34.

(12) Eisenberg, D.; Jucker, M. The amyloid state of proteins in human diseases. *Cell* **2012**, *148* (6), 1188−203.

(13) Owen, M. C.; Gnutt, D.; Gao, M.; Wärmländer, S. K. T. S.; Jarvet, J.; Gräslund, A.; Winter, R.; Ebbinghaus, S.; Strodel, B. Effects of in vivo conditions on amyloid aggregation. *Chem. Soc. Rev.* **2019**, *48* (14), 3946−3996.

(14) Cline, E. N.; Bicca, M. A.; Viola, K. L.; Klein, W. L. The Amyloid-beta Oligomer Hypothesis: Beginning of the Third Decade. *J. Alzheimers Dis* **2018**, *64* (s1), S567−S610.

(15) Yang, J.; Perrett, S.; Wu, S. Single Molecule Characterization of Amyloid Oligomers. *Molecules* **2021**, *26* (4), 948.

(16) Gambardella, C.; Offi, C.; Patrone, R.; Clarizia, G.; Mauriello, C.; Tartaglia, E.; Di Capua, F.; Di Martino, S.; Romano, R. M.; Fiore, L.; Conzo, A.; Conzo, G.; Docimo, G. Calcitonin negative Medullary

Thyroid Carcinoma: a challenging diagnosis or a medical dilemma? *BMC Endocr Disord* **2019**, *19* (Suppl 1), 45.
(17) Pelizzo, M. R.; Torresan, F.; Da Roit, A.; Merante Boschin, I.; Chondrogiannis, S.; Rampin, L.; Colletti, P. M.; Vinjamury, S.; Perkins, A. J.; Rubello, D. Mild to moderate increase of serum calcitonin levels only in presence of large medullary thyroid cancer deposits. *Rev. Esp Med. Nucl. Imagen Mol.* **2015**, *34* (6), 378−382.
(18) Khurana, R.; Agarwal, A.; Bajpai, V. K.; Verma, N.; Sharma, A. K.; Gupta, R. P.; Madhusudan, K. P. Unraveling the amyloid associated with human medullary thyroid carcinoma. *Endocrinology* **2004**, *145* (12), 5465−70.
(19) Belfiore, M.; Cariati, I.; Matteucci, A.; Gaddini, L.; Macchia, G.; Fioravanti, R.; Frank, C.; Tancredi, V.; D'Arcangelo, G.; Diociaiuti, M. Calcitonin native prefibrillar oligomers but not monomers induce membrane damage that triggers NMDA-mediated Ca(2+)-influx, LTP impairment and neurotoxicity. *Sci. Rep* **2019**, *9* (1), 5144.
(20) Wärmländer, S. K. T. S.; Tiiman, A.; Abelein, A.; Luo, J.; Jarvet, J.; Söderberg, K. L.; Danielsson, J.; Gräslund, A. Biophysical studies of the amyloid beta-peptide: interactions with metal ions and small molecules. *Chembiochem* **2013**, *14* (14), 1692−704.
(21) Wu, D.; Doods, H.; Arndt, K.; Schindler, M. Development and potential of non-peptide antagonists for calcitonin-gene-related peptide (CGRP) receptors: evidence for CGRP receptor heterogeneity. *Biochem. Soc. Trans.* **2002**, *30* (4), 468−73.
(22) Du, H.-N.; Ding, J.-G.; Cui, D.-F.; Hu, H.-Y. Novel Secondary Structure of Calcitonin in Solid State as Revealed by Circular Dichroism Spectroscopy. *Chin. J. Chem.* **2002**, *20* (7), 697−698.
(23) Arvinte, T.; Cudd, A.; Drake, A. F. The structure and mechanism of formation of human calcitonin fibrils. *J. Biol. Chem.* **1993**, *268* (9), 6415−22.
(24) Johansson, E.; Hansen, J. L.; Hansen, A. M.; Shaw, A. C.; Becker, P.; Schaffer, L.; Reedtz-Runge, S. Type II Turn of Receptor-bound Salmon Calcitonin Revealed by X-ray Crystallography. *J. Biol. Chem.* **2016**, *291* (26), 13689−98.
(25) Greenfield, N. J. Using circular dichroism spectra to estimate protein secondary structure. *Nat. Protoc* **2006**, *1* (6), 2876−90.
(26) Jarvet, J. *Nuclear Magnetic Resonance Studies of Peptide Structure and Dynamics*; Doctoral Dissertation; Stockholm University: Stockholm, Sweden, 1999.
(27) Kelly, S. M.; Jess, T. J.; Price, N. C. How to study proteins by circular dichroism. *Biochim. Biophys. Acta* **2005**, *1751* (2), 119−39.
(28) Whitmore, L.; Wallace, B. A. Protein secondary structure analyses from circular dichroism spectroscopy: methods and reference databases. *Biopolymers* **2008**, *89* (5), 392−400.
(29) Micsonai, A.; Moussong, E.; Wien, F.; Boros, E.; Vadaszi, H.; Murvai, N.; Lee, Y. H.; Molnar, T.; Refregiers, M.; Goto, Y.; Tantos, A.; Kardos, J. BeStSel: webserver for secondary structure and fold prediction for protein CD spectroscopy. *Nucleic Acids Res.* **2022**, *50* (W1), W90−W98.
(30) Wiedemann, C.; Bellstedt, P.; Gorlach, M. CAPITO-a web server-based analysis and plotting tool for circular dichroism data. *Bioinformatics* **2013**, *29* (14), 1750−7.
(31) Miles, A. J.; Wallace, B. A. CDtoolX, a downloadable software package for processing and analyses of circular dichroism spectroscopic data. *Protein Sci.* **2018**, *27* (9), 1717−1722.
(32) Danielsson, J.; Jarvet, J.; Damberg, P.; Gräslund, A. The Alzheimer beta-peptide shows temperature-dependent transitions between left-handed 3-helix, beta-strand and random coil secondary structures. *FEBS J.* **2005**, *272* (15), 3938−49.
(33) Kelly, M. A.; Chellgren, B. W.; Rucker, A. L.; Troutman, J. M.; Fried, M. G.; Miller, A. F.; Creamer, T. P. Host-guest study of left-handed polyproline II helix formation. *Biochemistry* **2001**, *40* (48), 14376−83.
(34) Uversky, V. N. A multiparametric approach to studies of self-organization of globular proteins. *Biochemistry (Mosc)* **1999**, *64* (3), 250−266.
(35) Micsonai, A.; Moussong, E.; Murvai, N.; Tantos, A.; Toke, O.; Refregiers, M.; Wien, F.; Kardos, J. Disordered-Ordered Protein Binary Classification by Circular Dichroism Spectroscopy. *Front Mol. Biosci* **2022**, *9*, 863141.
(36) Yang, J. T.; Kubota, S.; Ordered Conformation of Poly(L-Lysine) and its Homologs in Anionic Surfactant Solutions. In *Microdomains in Polymer Solutions*; Dubin, P., Ed.; Springer: New York, 1985; pp 311−331.
(37) Balcerski, J. S.; Pysh, E. S.; Bonora, G. M.; Toniolo, C. Vacuum ultraviolet circular dichroism of beta-forming alkyl oligopeptides. *J. Am. Chem. Soc.* **1976**, *98* (12), 3470−3.
(38) Smith, L. J.; Fiebig, K. M.; Schwalbe, H.; Dobson, C. M. The concept of a random coil. Residual structure in peptides and denatured proteins. *Fold Des* **1996**, *1* (5), R95−106.
(39) Drake, A. F.; Siligardi, G.; Gibbons, W. A. Reassessment of the electronic circular dichroism criteria for random coil conformations of poly(L-lysine) and the implications for protein folding and denaturation studies. *Biophys Chem.* **1988**, *31* (1−2), 143−6.
(40) Adzhubei, A. A.; Sternberg, M. J.; Makarov, A. A. Polyproline-II helix in proteins: structure and function. *J. Mol. Biol.* **2013**, *425* (12), 2100−32.
(41) Narwani, T. J.; Santuz, H.; Shinada, N.; Melarkode Vattekatte, A.; Ghouzam, Y.; Srinivasan, N.; Gelly, J. C.; de Brevern, A. G. Recent advances on polyproline II. *Amino Acids* **2017**, *49* (4), 705−713.
(42) Österlund, N.; Kulkarni, Y. S.; Misiaszek, A. D.; Wallin, C.; Kruger, D. M.; Liao, Q.; Mashayekhy Rad, F.; Jarvet, J.; Strodel, B.; Wärmländer, S. K. T. S.; Ilag, L. L.; Kamerlin, S. C. L.; Gräslund, A. Amyloid-beta Peptide Interactions with Amphiphilic Surfactants: Electrostatic and Hydrophobic Effects. *ACS Chem. Neurosci.* **2018**, *9* (7), 1680−1692.
(43) Kjaergaard, M.; Norholm, A. B.; Hendus-Altenburger, R.; Pedersen, S. F.; Poulsen, F. M.; Kragelund, B. B. Temperature-dependent structural changes in intrinsically disordered proteins: formation of alpha-helices or loss of polyproline II? *Protein Sci.* **2010**, *19* (8), 1555−64.
(44) Gielnik, M.; Szymanska, A.; Dong, X.; Jarvet, J.; Svedruzic, Z. M.; Graslund, A.; Kozak, M.; Warmlander, S. Prion Protein Octarepeat Domain Forms Transient beta-Sheet Structures upon Residue-Specific Binding to Cu(II) and Zn(II) Ions. *Biochemistry* **2023**, *62* (11), 1689−1705.
(45) Österlund, N.; Luo, J.; Wärmländer, S. K. T. S.; Gräslund, A. Membrane-mimetic systems for biophysical studies of the amyloid-beta peptide. *Biochim Biophys Acta Proteins Proteom* **2019**, *1867* (5), 492−501.
(46) Wahlström, A.; Hugonin, L.; Peralvarez-Marin, A.; Jarvet, J.; Gräslund, A. Secondary structure conversions of Alzheimer's Abeta(1−40) peptide induced by membrane-mimicking detergents. *FEBS J.* **2008**, *275* (20), 5117−28.
(47) Vosough, F.; Barth, A. Characterization of Homogeneous and Heterogeneous Amyloid-beta42 Oligomer Preparations with Biochemical Methods and Infrared Spectroscopy Reveals a Correlation between Infrared Spectrum and Oligomer Size. *ACS Chem. Neurosci.* **2021**, *12* (3), 473−488.
(48) Lau, S. Y.; Taneja, A. K.; Hodges, R. S. Synthesis of a model protein of defined secondary and quaternary structure. Effect of chain length on the stabilization and formation of two-stranded alpha-helical coiled-coils. *J. Biol. Chem.* **1984**, *259* (21), 13253−61.
(49) Zhou, N. E.; Kay, C. M.; Hodges, R. S. Synthetic model proteins: the relative contribution of leucine residues at the nonequivalent positions of the 3−4 hydrophobic repeat to the stability of the two-stranded alpha-helical coiled-coil. *Biochemistry* **1992**, *31* (25), 5739−46.
(50) Zhou, N. E.; Kay, C. M.; Hodges, R. S. Synthetic model proteins. Positional effects of interchain hydrophobic interactions on stability of two-stranded alpha-helical coiled-coils. *J. Biol. Chem.* **1992**, *267* (4), 2664−70.
(51) Barbar, E.; Nyarko, A. NMR Characterization of Self-Association Domains Promoted by Interactions with LC8 Hub Protein. *Comput. Struct Biotechnol J.* **2014**, *9*, No. e201402003.
(52) Berntsson, E.; Vosough, F.; Svantesson, T.; Pansieri, J.; Iashchishyn, I. A.; Ostojic, L.; Dong, X.; Paul, S.; Jarvet, J.; Roos, P.


https://doi.org/10.1021/acsomega.4c05312
*ACS Omega* 2025, 10, 17133−17142

M.; Barth, A.; Morozova-Roche, L. A.; Graslund, A.; Warmlander, S. Residue-specific binding of Ni(II) ions influences the structure and aggregation of amyloid beta (Abeta) peptides. *Sci. Rep* **2023**, *13* (1), 3341.
(53) Tiiman, A.; Luo, J.; Wallin, C.; Olsson, L.; Lindgren, J.; Jarvet, J.; Per, R.; Sholts, S. B.; Rahimipour, S.; Abrahams, J. P.; Karlström, A. E.; Gräslund, A.; Wärmländer, S. K. T. S. Specific Binding of Cu(II) Ions to Amyloid-Beta Peptides Bound to Aggregation-Inhibiting Molecules or SDS Micelles Creates Complexes that Generate Radical Oxygen Species. *J. Alzheimers Dis* **2016**, *54* (3), 971−982.
(54) Wüthrich, K. *NMR in biological research: Peptides and proteins*; North-Holland Publishing Company: Amsterdam, Holland, 1976; pp 65−72.
(55) Kamihira, M.; Naito, A.; Tuzi, S.; Nosaka, A. Y.; Saito, H. Conformational transitions and fibrillation mechanism of human calcitonin as studied by high-resolution solid-state 13C NMR. *Protein Sci.* **2000**, *9* (5), 867−77.
(56) Arvinte, T.; Drake, A. F. Comparative study of human and salmon calcitonin secondary structure in solutions with low dielectric constants. *J. Biol. Chem.* **1993**, *268* (9), 6408−14.
(57) Siligardi, G.; Samori, B.; Melandri, S.; Visconti, M.; Drake, A. F. Correlations between biological activities and conformational properties for human, salmon, eel, porcine calcitonins and Elcatonin elucidated by CD spectroscopy. *Eur. J. Biochem.* **1994**, *221* (3), 1117−25.
(58) Motta, A.; Pastore, A.; Goud, N. A.; Castiglione Morelli, M. A. Solution conformation of salmon calcitonin in sodium dodecyl sulfate micelles as determined by two-dimensional NMR and distance geometry calculations. *Biochemistry* **1991**, *30* (43), 10444−50.
(59) Motta, A.; Castiglione Morelli, M. A.; Goud, N.; Temussi, P. A. Sequential 1H NMR assignment and secondary structure determination of salmon calcitonin in solution. *Biochemistry* **1989**, *28* (20), 7996−8002.
(60) Motta, A.; Temussi, P. A.; Wunsch, E.; Bovermann, G. A 1H NMR study of human calcitonin in solution. *Biochemistry* **1991**, *30* (9), 2364−71.
(61) Renawala, H. K.; Chandrababu, K. B.; Topp, E. M. Fibrillation of Human Calcitonin and Its Analogs: Effects of Phosphorylation and Disulfide Reduction. *Biophys. J.* **2021**, *120* (1), 86−100.
(62) Mitra, A.; Paul, S. Pathways of hLL-37(17−29) Aggregation Give Insight into the Mechanism of alpha-Amyloid Formation. *J. Phys. Chem. B* **2023**, *127* (38), 8162−8175.
(63) Jayaraman, M.; Kodali, R.; Sahoo, B.; Thakur, A. K.; Mayasundari, A.; Mishra, R.; Peterson, C. B.; Wetzel, R. Slow amyloid nucleation via alpha-helix-rich oligomeric intermediates in short polyglutamine-containing huntingtin fragments. *J. Mol. Biol.* **2012**, *415* (5), 881−99.
(64) Liu, Y.; Wang, Y.; Zhang, Y.; Zou, Y.; Wei, G.; Ding, F.; Sun, Y. Structural Perturbation of Monomers Determines the Amyloid Aggregation Propensity of Calcitonin Variants. *J. Chem. Inf Model* **2023**, *63* (1), 308−320.
(65) Nakamuta, H.; Orlowski, R. C.; Epand, R. M. Evidence for calcitonin receptor heterogeneity: binding studies with nonhelical analogs. *Endocrinology* **1990**, *127* (1), 163−9.
(66) Wärmländer, S. K. T. S.; Österlund, N.; Wallin, C.; Wu, J.; Luo, J.; Tiiman, A.; Jarvet, J.; Gräslund, A. Metal binding to the amyloid-beta peptides in the presence of biomembranes: potential mechanisms of cell toxicity. *J. Biol. Inorg. Chem.* **2019**, *24* (8), 1189−1196.
(67) Rocha, S.; Loureiro, J. A.; Brezesinski, G.; Pereira, M. d. C. Peptide-surfactant interactions: consequences for the amyloid-beta structure. *Biochem. Biophys. Res. Commun.* **2012**, *420* (1), 136−140.
(68) Kitamata, M.; Inaba, T.; Suetsugu, S. The roles of the diversity of amphipathic lipids in shaping membranes by membrane-shaping proteins. *Biochem. Soc. Trans.* **2020**, *48* (3), 837−851.
(69) Vorobyov, I.; Allen, T. W. On the role of anionic lipids in charged protein interactions with membranes. *Biochim. Biophys. Acta* **2011**, *1808* (6), 1673−83.
(70) Wang, Y.; Majd, S. Charged Lipids Modulate the Phase Separation in Multicomponent Membranes. *Langmuir* **2023**, *39* (32), 11371−11378.


https://doi.org/10.1021/acsomega.4c05312
*ACS Omega* 2025, 10, 17133−17142